Yarn-level modelling and geometric simulation of warp-knitted clothing elements – first results and challenges

Haisang Liu[1,2,*], Yordan Kyosev[2], Gaoming Jiang[1]

[1]*Jiangnan University, Wuxi, China*
[2] *TU Dresden, Dresden, Germany*

Corresponding author E-mail address: sophie@stu.jiangnan.edu.cn

INFO

ABSTRACT

To simulate a warp-knitted product with a specific shape, a mesh-based model for modeling and simulation is proposed. The three-dimensional geometry of the final fabric is represented as a set of polygons, each of them containing information about the 3D orientation of the yarns in the warp knitted structure. Using spatial mapping, stitch coordinates are transformed from the flat mesh model to the three-dimensional mesh model and the final rendering is accomplished. The method provides yarn level data for the complete structure and can be used for speeding up the design process of clothing with warp-knitted products. Several challenges with the larger data amount and possible ways for their solutions are discussed.

1   Introduction

When designing warp-knitted products, it is necessary to check the pattern and appearance through repeated proofing. Owing to the complexity of the knitting process and interlocking stitches, the simulated fabric is described by modeling the stitch with knitting parameters. The parameters can be modified after seeing the simulated structure during design, which is a time-saving and material-saving method to shorten the design process.

As one of the hot spots in the textile field, effective fabric simulation was widely used in clothing animation [1]. Fabric dynamic performance such as draping and wrinkle was imitated using finite elements, a particle system and other methods [2-3]. Although fabric stress was well expressed, the specific structure of the fabrics was not perfectly presented. Combined with the knitting structure, several

loop shapes were simulated using an interlacing point-based model. The interpolation method was applied to the yarn texture mapping and 2D (two dimensional) pattern simulation was realized [4-5]. Li et al. [6-7] extracted the illumination function from scanned yarns for Jacquardtronic lace and a mass-spring model was used for yarn deformation. Analyzing the warp-knitted structure, underlaps and overlaps were put into several layers, which were piled up together to simulate patterns [8]. However, the above appearance simulation methods for knitted fabrics were all in the 2D hierarchy. The 3D (three-dimensional) structure of fabrics and stitches was not reflected.

The 3D simulation of stitches is more complex than that of the visual pattern because yarn paths need to be defined corresponding to knitting parameters. Many scholars have modeled the stitch shape based on actual measurements [9-10]. The mass-spring system was also used to describe stitch deformation caused by internal forces [11-12]. In addition, the stitch position of a warp-knitted spacer fabric with different thicknesses was calculated by a mathematical method [13]. A similar method was used to simulate a tubular warp-knitted fabric with regular radii [14]. But these methods were suitable for fabric with regular tubes rather than fabrics with arbitrary shapes.

To solve the problem of fabric simulation with complex surfaces, many researchers focused on 3D geometry modeling. Igarashi et al. [15] meshed a 3D model into hundreds of triangles and quadrilaterals, which were filed separately with corresponding weft structures. Yuksel et al. [16] put finer meshes on the clothing model. The multiple stitch types were assigned to those meshes so that the complicated knitting patterns could be imitated. Similarly, arbitrary 3D shapes were converted to knit models with valid stitch meshes according to the knitted structure [17]. Various shapes with defined wales edges or course edges were proposed and a new structure was introduced by Wu et al. [18] to represent knitting short rows. Araújo et al. [19] proposed a 2D hexagonal structure related to non-linear truss elements to simulate the weft structure. Using this method, the elongation deformation in one or more directions was simulated. Experimental results also showed that it worked well for a spherical shape in 3D case. Distinguished from the weft structures mentioned above, stitch interlocking structures are redefined in the warp-knitted fabric, leading to different ways for meshing and modeling.

In this paper, we propose an effective modeling and simulation method for warp-knitted fabric with 3D stitches. The stitch model and structure mesh are modeled according to parameters. The fabric mesh is input as the basis of the 3D shape of the fabric. A coordinate space conversion relationship is found to translate the coordinate from a flat fabric to a 3D product, which can properly handle the stitch position on the 3D model. A simulation method combining model processing and yarn rendering is proposed to realize the visual design for warp-knitted fabric with complex structures.

2 Mesh model
2.1 Stitch model

The stitch is the basic structural unit of forming the warp-knitted fabric, where the bent yarn is divided into overlaps and underlaps. As can be seen from Figure 1, the top of the current-course stitch is formed by overlap interlocks with the bottom of the next-course stitch. Stitches in the same yarn are connected by underlaps that can be seen from the fabric back. This relationship determines that one stitch can be put in a frame model with two control points, where each point controls several stitches in series.
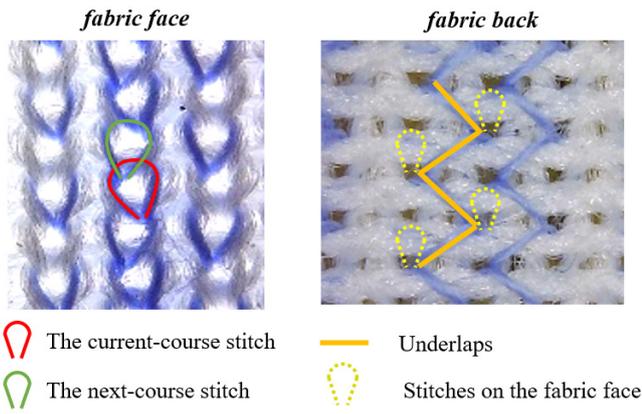
Fig. 1   The stitch interlocking relationship.
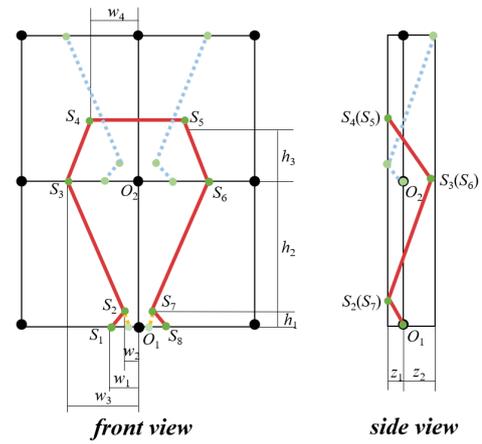
Fig. 2   Stitch model.

Referring to actual measurements [8], the stitch dimension is determined. 8 data points are introduced to describe the 3D stitch shape as shown in Figure 2. The red stitch is at the current course and the blue one is at the next course. O_1 and O_2 control the stitch position and $S_1 \sim S_8$ are 8 data points to control the stitch shape. Due to the uncertain position of the next stitch, left, right or at the same wale, two bottom points S_1 and S_8 are determined by the direction of underlaps as orange lines show. Although the stitch shape as well as the position of two control points O_1 and O_2 will change resulting from internal forces, the dynamic relationship between control points and data points remains unchanged. $w_1 \sim w_4$ are lateral distances from the longitudinal axis. $h_1 \sim h_3$ are longitudinal dimension. z_1 and z_2 are dimensions of stitch thickness.

2.2   Structure mesh

Stitches are arranged regularly in the fabric. Combined with the stitch model in four squares, a structure mesh, regarded as the geometric abstraction of a plane fabric, is proposed to enable easier modeling. The fabric is attached to the mesh model, where the mesh vertices coincide with the stitch control points. For most normal fabrics, the mesh size depends on the fabric pattern. As shown in Fig. 3(a), the structure mesh is divided into two parts. The right pink grids are occupied by stitches within pattern width, while the left blue grids are covered by stitches of the last yarn beyond pattern width. The stitch model shown in Fig. 2 reveals that four grids are involved in one stitch with 3*3 vertices. Therefore, auxiliary vertices are arranged at the edges of the structure mesh as shown in Fig. 3(b). Pink vertices are directly linked to control points. So for this structure in Figure 3, although the pattern is 4 wales and 4 courses, the structure mesh is in the size of 8 wales and 5 courses. The grid size is decided by the fabric density.
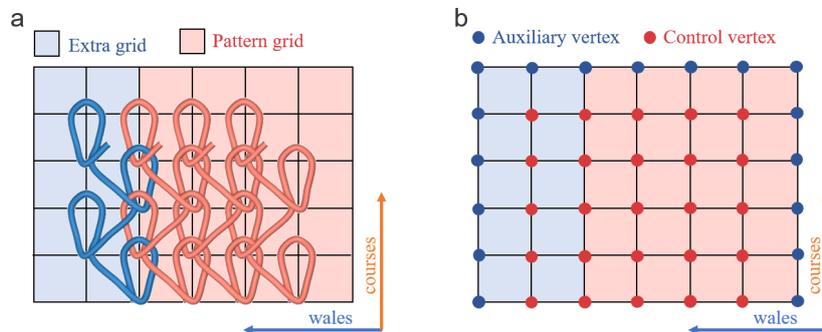
Fig. 3   Structure mesh: (a) stitches arranged in the fabric; (b) structure mesh with vertices.

2.3   Fabric mesh

A group of 3D models including a plane mesh and a curved-surface mesh is needed in our simulation method. The two models correspond to each other at the parameter level. The final simulated shape of

117

the fabric is limited to the curved-surface mesh. To achieve this goal, the mature commercial software Clo3D is used. A fabric mesh, output in obj format, contains parameters such as vertex, face, vector and so on. The fabric mesh is divided into triangles. The triangle on the plane mesh match with that on the curved-surface model, having the same indexes and different vertex and vectors. Figure 4 shows a group of fabric meshes.

Plane model   Curved-surface model
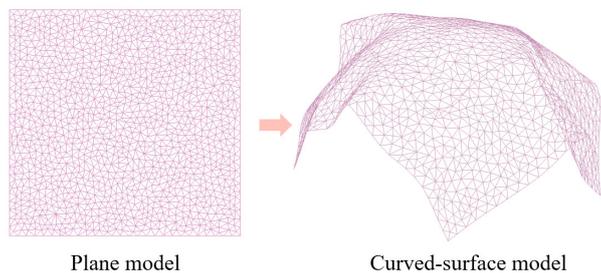
Fig. 4   Fabric meshes.

3   Coordinate calculation

The plane model is a medium connecting the structure mesh and the curved-surface mesh. As shown in Figure 5, a plane mesh is overlapped by a structure mesh, through which the grid size and the pattern size matching the fabric mesh can be obtained. A detailed unit is extracted showing data point distribution. Triangles belonging to four quadrilaterals are traversed to determine the point ascription, preparing for the coordinate transformation.

Mesh model   Stitch model
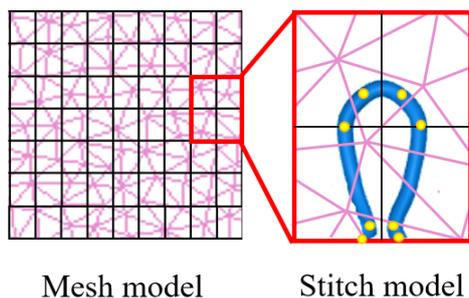
Fig. 5   Relationship between a structure mesh and a fabric mesh.

3.1   Data point attribution

It is necessary to match the data points to the fabric mesh with triangles to locate the stitch on the fabric. The triangle index is added into data point attribution, as visible in Figure 6. Generally, most data points are inside the triangle, as shown in Figure 6a. Sometimes in particular the data point is exactly on the edge or vertex of the triangle (cf. Figure 6b and c), which indicates that this data point belongs to more than one triangle. Thus, the first matched triangle is selected to avoid repeated calculation.

(a)   (b)   (c)
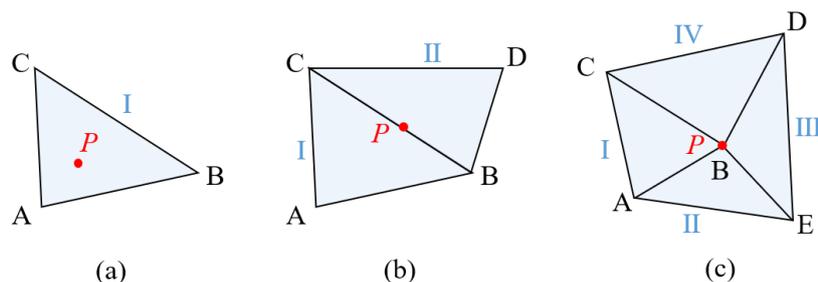
Fig. 6   Data point attribution: (a) inside the triangle; (b) on the triangle edge; (c) on the triangle vertex.

In Figure 6(a), P is one of the stitch data points. A, B and C are three vertexes of the triangle on the plane fabric mesh. As shown in Equation (1), vectors from P to three vertexes ($\overrightarrow{PA}$, $\overrightarrow{PB}$ and $\overrightarrow{PC}$) are calculated for the cross product based on pairwise combinatorial.

$$\begin{cases} t_1 = |\overrightarrow{PA}||\overrightarrow{PB}| \sin \theta_1 \\ t_2 = |\overrightarrow{PA}||\overrightarrow{PC}| \sin \theta_2, \\ t_3 = |\overrightarrow{PB}||\overrightarrow{PC}| \sin \theta_3 \end{cases} \qquad (1)$$

where t_1, t_2 and t_3 are the values of three cross-product equations, $\overrightarrow{PA}$, $\overrightarrow{PB}$ and $\overrightarrow{PC}$ are three vectors from P to three vertexes, and θ_1, θ_2 and θ_3 are angles between the vectors.

The triangle index is decided by these values. If one of the following conditions is satisfied, it can be judged that P is inside the triangle. The judgment conditions are as follows: $t_1>0$, $t_2>0$ and $t_3>0$, or $t_1<0$, $t_2<0$ and $t_3<0$. When P is on the triangle edge or the vertex, two or more triangles meet the requirement. To ensure the singularity of the triangle ascription, the triangle that has the smaller index is selected to be recorded.

3.2   Point spatial mapping

The curved-surface mesh is evolved from the plane mesh whose triangles have a spatial relationship with the same index. Figure 7 shows the coordinate spatial mapping from the triangle on the plane mesh ($\triangle$ABC) to that on the curved-surface mesh ($\triangle$A'B'C'). Based on the triangle vectors, a space mapping relationship between $\triangle$ABC and $\triangle$A'B'C' is established. Two matrices with 4×4 size are used to describe the spatial information of two triangles: M_1 (Eq. (2)) for $\triangle$ABC and M_2 (Eq. (3)) for $\triangle$A'B'C'.
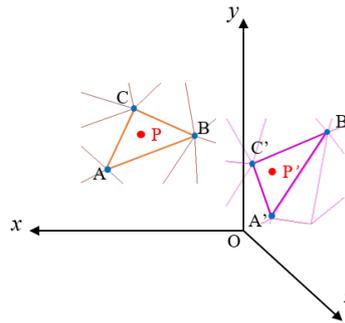
Fig. 7   Coordinate spatial mapping.

$$M_1 = \begin{bmatrix} \overrightarrow{AB}.x & \overrightarrow{AC}.x & \overrightarrow{AB} \times \overrightarrow{AC}.x & A.x \\ \overrightarrow{AB}.y & \overrightarrow{AC}.y & \overrightarrow{AB} \times \overrightarrow{AC}.y & A.y \\ \overrightarrow{AB}.z & \overrightarrow{AC}.z & \overrightarrow{AB} \times \overrightarrow{AC}.z & A.z \\ 0 & 0 & 0 & 1 \end{bmatrix} \qquad (2)$$

$$M_2 = \begin{bmatrix} \overrightarrow{A'B'}.x & \overrightarrow{A'C'}.x & \overrightarrow{A'B'} \times \overrightarrow{A'C'}.x & A'.x \\ \overrightarrow{A'B'}.y & \overrightarrow{A'C'}.y & \overrightarrow{A'B'} \times \overrightarrow{A'C'}.y & A'.y \\ \overrightarrow{A'B'}.z & \overrightarrow{A'C'}.z & \overrightarrow{A'B'} \times \overrightarrow{A'C'}.z & A'.z \\ 0 & 0 & 0 & 1 \end{bmatrix} \qquad (3)$$

$$M = M_1 \times M_2^{-1} \qquad (4)$$

$$P' = M \times P \qquad (5)$$

where A is one of the vertexes, $\overrightarrow{AB}$ and $\overrightarrow{AC}$ are two edge vectors of $\triangle$ABC containing vertex A, their x-value, y-value and z-value are shown in Equation (2). Similarly, information of one vertex and two edge vectors of $\triangle$A'B'C' are shown in Equation (3). From the equations above, the spatial coordinate mapping matrix is shown as Equation (4). M_2^{-1} is the inverse matrix of M_2. P is the initial point on the plane mesh and P' is the transformed point on the curved-surface mesh (Equation (5)).

In this way, all points of stitches arranged flatly on the plane mesh are transformed and the final stitch position on the curved-surface mesh is determined.

4 Rendering implementation
4.1   Tube parameters

Data points are connected using tube geometry encapsulated in Three.js and virtual yarns are simulated. Three.js is a cross-browser JavaScript library and application programming interface (API) used to create and display animated 3D computer graphics in a web browser using WebGL. There are five key parameters to support the tube establishment: path, tubular segments, radius, section edge number and closeness. The path is determined by the shape-controlling points, the radius is decided by the input parameters of yarn specification and the tube is defaulted to open. Tubular segments and section edge numbers decide the tube smoothness. A lot of data calculation of tube surface will increase rendering load, even cause the rendering crash. Thus, tubular segments (S_t) and section edge number (S_r) should be defined according to the actual visual effect and the running time.

Figure 8 shows a group of tubes with section edge numbers (S_r) from 3 to 13 with a step of 2. The tube section gets rounder as S_r increases. The number of vertexes, as well as rendering time, also increases with the increase of S_r. Therefore, S_r is limited within a reasonable range, ensuring the fabric has an appropriate visual appearance and rendering time.
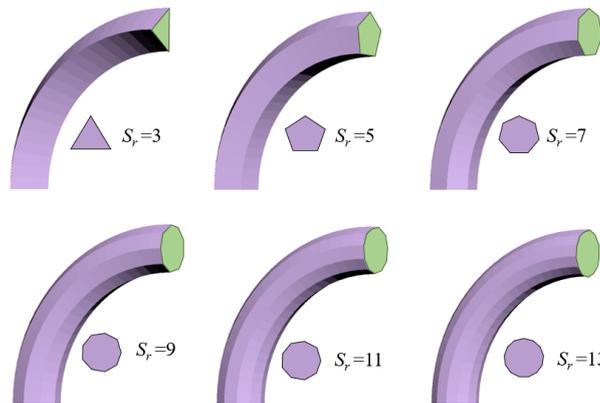
Fig. 8   Yarn tubes with different section edge numbers (S_r).

Figure 9 shows several tubes with different tubular segments (S_t) under S_r=11 between two points. It is visible that the larger the S_t is, the smoother the tube looks. There is no significant visual difference when S_t is large enough.

Considering the longer running time with the finer surface rendering, the tube parameters are chosen according to the visual effect and running memory, which is directly reflected in the stitch quantity. The tube faces are restricted within the maximum level with a reasonable appearance to avoid rendering crash results from the large calculation.
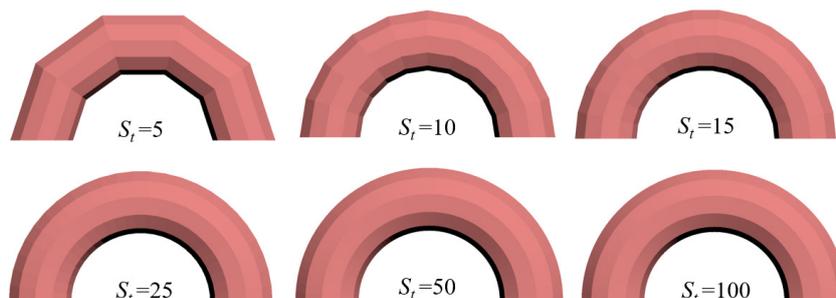
Fig. 9   Yarn tubes with several tubular segments (S_t).

4.2   Texture mapping

The real-world yarn is usually a fiber bundle. Considering the amount of calculation, not all fibers can be modeled. Hence, a texture mapping method based on PBR (Physically Based Rendering) is applied to simulate the yarn appearance. A quadrilateral-continuity texture ensures that the pattern has a seamless and continuous connection rendered on the yarn. The parameters (u, v) express the texture vertex coordinate at horizontal and longitudinal directions. Assuming that vertices of a pattern unit are (0,0), (0,1), (1,0) and (1,1), the texture coordinates of the yarn tube can be derived from Equation (6).

$$\begin{cases} u_s = s/S_r \\ v_s = e \times l \end{cases} \tag{6}$$

where S_r is the section edge number and s is the sth vertex, u_s is the sth horizontal component, l is the length of one tube segment, e is the mapping coefficient, and v_s is the sth longitudinal component.

5   Results and discussion

The simulation process of warp-knitted fabrics is shown in Figure 10. The structure mesh is established according to the knitting parameters. The mass-spring model is used [8] to describe the stitch deformation and the data points are calculated. Finally, based on the coordinate spatial relationship, stitches on the curved-surface model are determined to realize the simulation.

Chain notation   Stitch model   Structure mesh   Fabric meshes   Simulated fabric
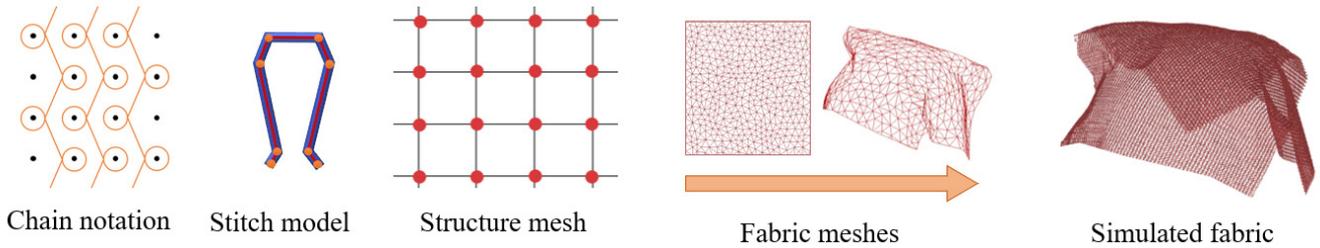
Fig. 10 Simulation process.

5.1   Simulation of warp-knitted fabrics

Figure 11(a) and (b) show simulation results of a tricot structure and a mesh structure from plane fabrics to 3D curved fabrics. And the comparison between colored tubes and yarn-surface tubes. The fully-formed products[14] shown in Figure 11(c) can also be simulated in this way. The geometric model proposed in this paper can accurately represent the shape of the fabrics.

a

Plane fabric   Curved fabric

Tricot structure

Pure tubes

Mapped surface

Fig. 11 Cont.

b

Plane fabric   Curved fabric

Mesh structure

c

Tube   Skirt
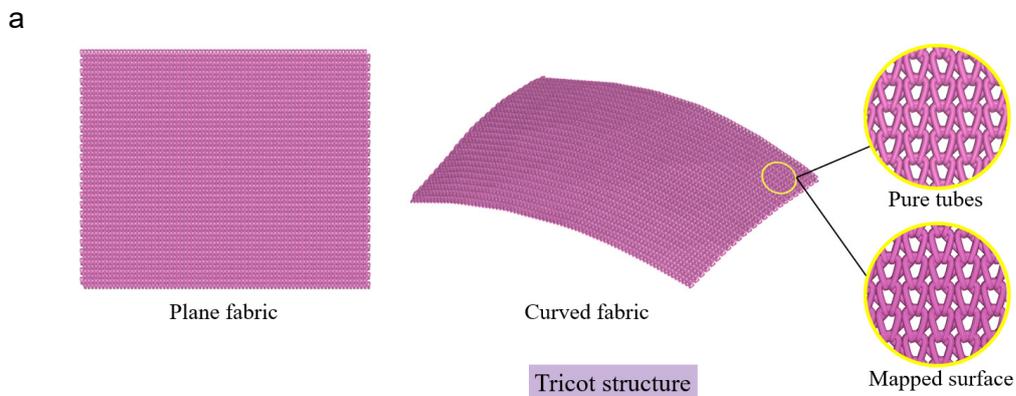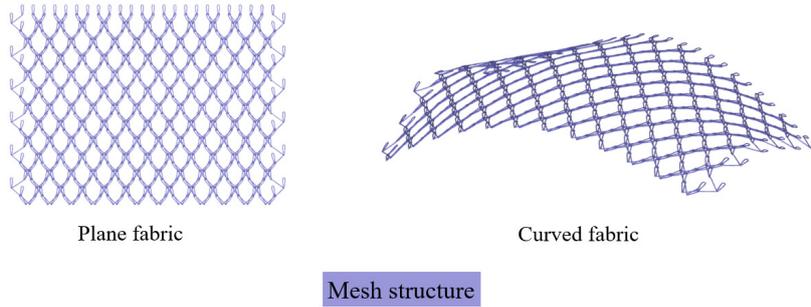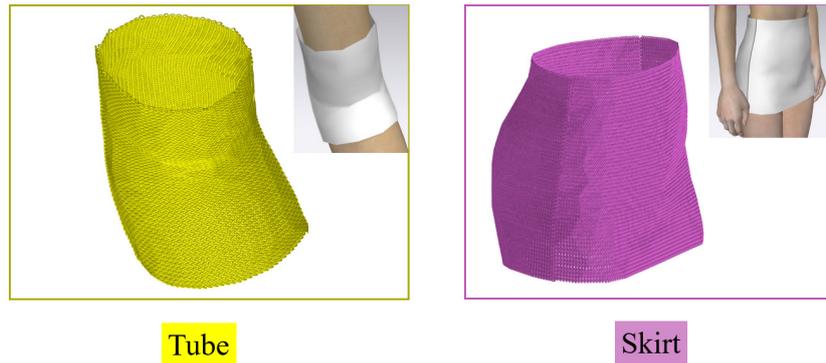
Fig. 11 Simulation results of warp structures: (a) tricot structure; (b) mesh structure; (c) warp-knitted products.

Sometimes, not all of the fabric surface tends to be flat. When the fabric is picked up, it has a strong curvature at the pinched place. Figure 12 shows both the loop-side and the underlap-side simulation results of a pinched fabric. The high curvature points have the same regular structure as the flat points, so that the method proposed in this paper fits the shape of the loops at points of strong curvature.

a
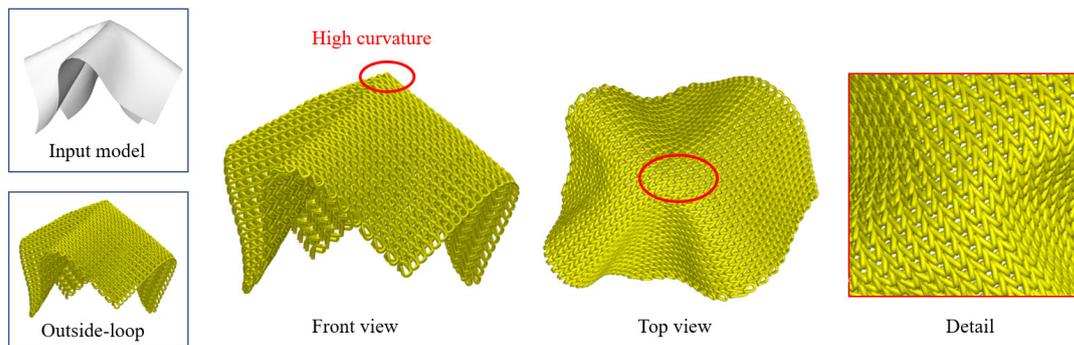
b
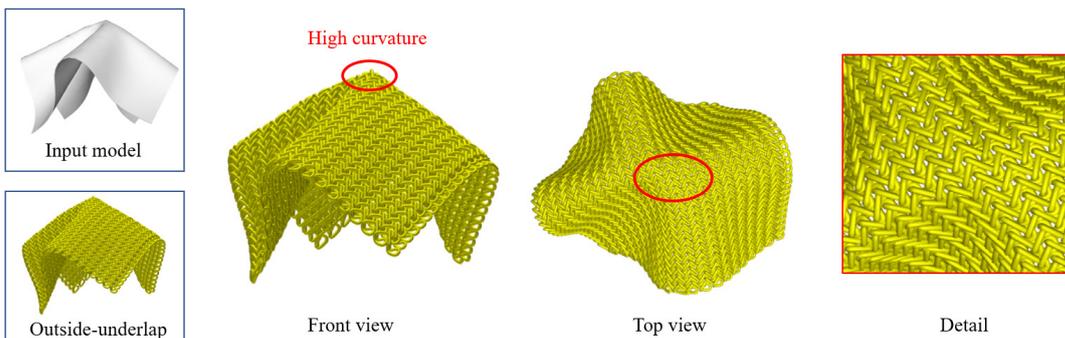
Fig. 12 Simulation results with high curvature: (a) details on loop side; (b) details on underlap side.

5.2 Simulation efficiency

The simulation is implemented in a Windows 10 system with 16 GB of RAM and an Intel Core i7-9750H CPU. C# is used to analyze the parameters and calculate point coordinates. WebGL technology is used to realize the rendering.

5.2.1 Tube parameters

Some common parameters are selected to simulate yarn tubes with reasonable appearances as shown in Figure 13. Corresponding rendering times with different fabric sizes (pattern width × pattern height) are shown in Figure 14. It is found that for the same fabric, the smoother the tube appearance is, the longer the rendering time is. Additionally, for the same parameters, the fabric with a larger pattern size takes a longer rendering time. This is closely related to the number of triangles consisting of yarn tubes in a stitch. Table 1 shows the parameter details. During the study, we also found that the overly specific appearance uses more memory, resulting in a rendering crash, especially for large size fabrics. Thus, it is necessary to select appropriate parameters according to the fabric size.

(a) (b) (c) (d) (e) (f)
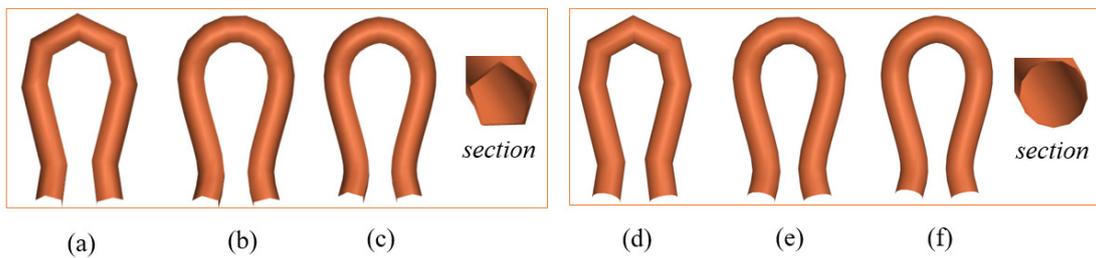
Fig. 13 Stitches with different tube parameters. (a) S_t =10, S_r =5; (b) S_t =25, S_r =5; (c) S_t =40, S_r =5; (d) S_t =10, S_r =13; (e) S_t =25, S_r =13; (f) S_t =40, S_r =13.
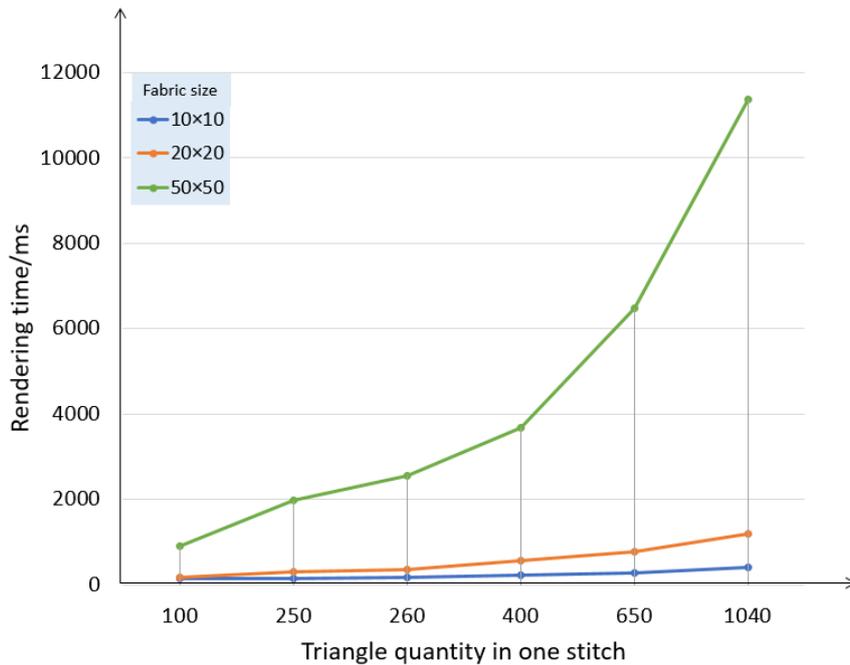
Fig. 14 Rendering time with several groups of tube parameters of different fabric size.

Table 1. Tube parameters and corresponding triangle quantity in one stitch

Tube parameters	S_t =10 S_r =5	S_t =25 S_r =5	S_t =40 S_r =5	S_t =10 S_r =13	S_t =25 S_r =13	S_t =40 S_r =13
Triangle quantity	100	250	400	260	650	1040

123

5.2.2 Texture mapping

Textures with a variety of sizes can be used to reflect the yarn surface. Figure 15 records the rendering times for several textures, where the control group uses the original tubes without texture mapping. The test fabric has a size of 10×10, using the parameters S_f=30 and S_r=13. Although texture mapping increases rendering time compared with the control group, the texture size does not cause significant fluctuations in rendering time. This is because the yarn superficial area keeps the same, once the stitch size and the yarn diameter are determined.
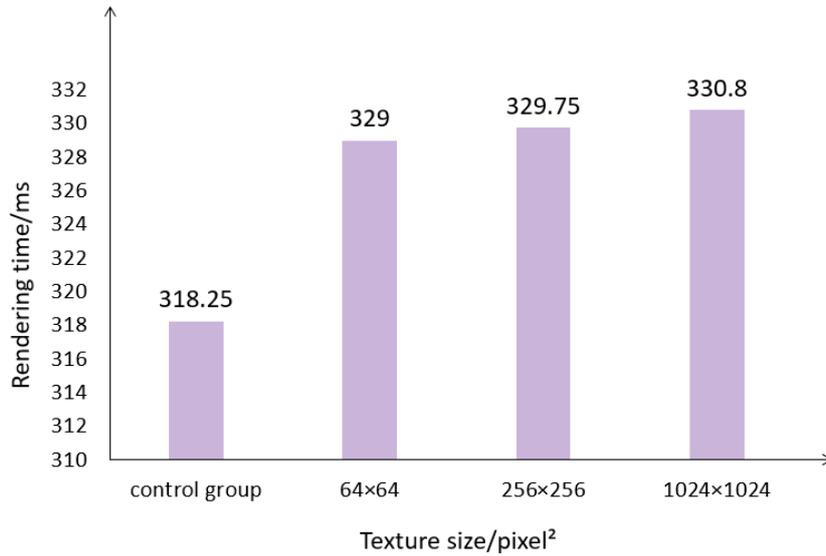
Fig. 15 The rendering time with texture mapping.

Table 2 is the running time of coordinate calculation for the fabrics shown in Figure 11. For the same fabric, the running time for the curved-surface fabric is longer than the plane fabric because of the extra coordinate mapping, which indicates that the method produced in this paper is efficient and useful.

Table 2. Running time of coordinate calculation.

	Stitch number	Plane running time (ms)	Curved-surface running time (ms)
Mesh fabric	576	41.46	58.35
Tricot fabric	3500	201.45	209.46
Tube	8480	496.52	521.08
Skirt	26180	1208.39	1375.15

5.3   Results comparison

At present, many scholars have carried out similar yarn-level three-dimensional simulations for warp knitted fabrics. In earlier studies, researchers defined the warp-knitted stitch shape using several control points, which are connected by NURBS curved lines [10,20]. The three-dimensional structure and modelling methods for warp-knitted fabrics were initially explored, but only idealized flat fabrics were simulated. Subsequently, Liu et al. [14] used mathematical methods to calculate the loop coordinates of regular tube fabrics to achieve a simple surface simulation. The method proposed in this paper not only covers these simple shapes, but also simulates the shapes of more complex warp knitted fabrics.

For other knitted fabrics, Yuksel et al. [16] and Wu et al. [17-18] directly meshed complex knitted fabric models. They preferred more detailed yarn-level simulation with yarn hairiness, which took more calculation and rendering time. Table 3 shows the running time comparison between Yuksel's method [16] and our method with similar stitch number. Texture maps are used to represent yarn surface patterns, we can use less time to simulate using lower capacity RAM (Yuksel: 48 GB RAM, ours: 16 GB

RAM). And in Yuksel's method, one stitch mesh contains one interlocking structure with one loop arc and several loop pillars, which is regarded as one stitch.

Table 3. Running time comparison.

No.	Yuksel		ours	
	Stich mesh	Running time	Stich	Running time
1	5373	1h	5400	4.42s
2	9976	1h	9996	7.43s
3	10220	2h	10400	7.80s
4	21568	7h	21600	15.56s

6 Conclusion

In this paper, a modeling and simulation method based on a mesh for curved-surface warp-knitted fabric is proposed. The fabric meshes including a plane mesh and a curved mesh produced by 3D modeling software are input. The spatial coordinate relationship between them is observed and the final coordinates are calculated. Texture mapping is introduced to simulate the yarn surface. The simulated results and simulation efficiency are analyzed. The results show that the higher precision parameters make smoother stitches, which also occupy more memory and rendering time. Moreover, the larger number of stitches causes the rendering to stop with an out-of-memory exception. So a reasonable tube parameter is significant for the stitch simulation. For the rapid-simulated fabrics, texture mapping to reflect the yarn surface is feasible to save memory and shorten the simulation time. Also, it is a problem that sometimes the simulation result has deficiency with interpenetrations of the tubes representing the yarn and has not been solved yet, which will be one of the research priorities and challenges of our future work in order to obtain better simulation results.

Author Contributions

Haisang Liu, methodology, formal analysis, software, writing – original draft preparation; Yordan Kyosev, supervision, writing – review and editing; Gaoming Jiang, resources, project administration. All authors have read and agreed to the published version of the manuscript.

Acknowledgements

Conflicts of Interest

The authors declare no conflict of interest.

References

1. Volino, P.; Magnenat-Thalmann, N.; Faure, F. A simple approach to nonlinear tensile stiffness for accurate cloth simulation. *ACM Trans. Graph.* **2019**, *28*(4), 105. DOI: 10.1145/1559755.1559762.
2. Wang, H. M.; O'Brien J. F.; Ramamoorthi, R. Data-driven elastic models for cloth: modeling and measurement. *ACM Trans. Graph.* **2011**, *30*(4), 1-12. DOI: 10.1145/2010324.1964966.
3. Wan, T. R.; Tang, W. Real-time computational modelling of textile fabric and cloth. *Journal of Xi'an Polytechnic University* **2013**, *27*(5), 551-562. DOI: 10.13338/j.issn.1674-649x.2013.05.007.
4. Lu, Z. W.; Jiang, G. M. Rapid simulation of flat knitting loops based on the yarn texture and loop geometrical model. *Autex Res. J.* **2017**, *17*(2), 103-110. DOI: 10.1515/aut-2016-0002.
5. Jiang, G. M.; Lu, Z. W.; Cong, H. L.; Zhang, A. J.; Dong, Z. J.; Jia. D. D. Flat knitting loop deformation simulation based on interlacing point model. *Autex Res. J.* **2017**, *17*(4), 361-369. DOI: 10.1515/aut-2016-0019.

6. Li, X. X.; Zhang, A. J.; Ma, P, B,; Cong, H. L.; Jiang, G. M. Structural deformation behavior of Jacquardtronic lace based on the mass-spring model. *Text. Res. J.* **2017**, *87*(10), 1242-1250. DOI: 10.1177/0040517516651103.
7. Li, X. X.; Jiang, G. M.; Zhang, A. J.; Chen, J. Y. A photograph-based approach for visual simulation of wrapped Jacquardtronic lace. *Text. Res. J.* **2018**, *88*(23), 2654-2664. DOI: 10.1177/0040517517729386.
8. Liu, H. S.; Jiang, G. M.; Dong, Z. J. A shortened development process method for warp-knitted yarn-dyed shirt fabric. *Text. Res. J.* **2021**, *91*(3-4), 443-455. DOI: 10.1177/0040517520937372.
9. Cong, H. L.; Ge, M. Q.; Jiang, G. M. 3-D modeling for warp knitted fabric based on NURBS. *Journal of Textile Research* **2008**, *11*, 132-136. DOI: 10.13475/j.fzxb.2008.11.003 (in Chinese).
10. Zhang, L. Z.; Jiang, G. M.; Gao, W. D. 3-D simulation and dynamic realization of warp-knitted structure. *Journal of Textile Research* **2009**, *30*(2), 125-129. DOI: 10.13475/j.fzxb.2009.02.011 (in Chinese).
11. Sha, S.; Ma, P. B.; Chapman, L. P.; Zhang, A. J. Three-dimensional modeling and simulation of deformation behavior of fancy weft knitted stitch fabric. *Text. Res. J.* **2017**, *87*(14), 1742-1751. DOI: 10.1177/0040517516658518.
12. Peng, J. J.; Jiang, G. M.; Xia, F. L.; Cong, H. L.; Dong, Z. J. Deformation and geometric modeling in three-dimensional simulation of fancy weft-knitted fabric. *Text. Res. J.* **2020**, *90*(13-14), 1527-1536. DOI: 10.1177/0040517519894749.
13. Renkens, W.; Kyosev, Y. Geometry modelling of warp knitted fabrics with 3D form. *Text. Res. J.* **2011**, *81*(4), 437-443. DOI: 10.1177/0040517510385171.
14. Liu, H. S.; Jiang, G. M.; Dong, Z. J. Mesh modeling and simulation for three-dimensional warp-knitted tubular fabrics. *J. Text. Inst.* **2021**, *113*(2), 301-313. DOI: 10.1080/00405000.2020.1871184.
15. Igarashi, Y.; Igarashi, T.; Suzuki, H. Knitting a 3D model. *Comput. Graph. Forum.* **2008**, *27*(7), 1737-1743. DOI: 10.1111/j.1467-8659.2008.01318.x.
16. Yuksel, C.; Kaldor, J. M.; James, D. L.; Marschner, S. Stitch meshes for modeling knitted clothing with yarn-level detail. *ACM Trans. Graph.* **2012**, *31*(4), 1-12. DOI: 10.1145/2185520.2185533.
17. Wu, K.; Gao, X.; Ferguson, Z.; Panozzo, D.; Yuksel C. Stitch meshing. *ACM Trans. Graph.* **2018**, *37*(4), 130. DOI: 10.1145/3197517.3201360.
18. Wu, K.; Swan, H.; Yuksel, C. Knittable stitch meshes. *ACM Trans. Graph.* **2019**, *38*(1), 10. DOI: 10.1145/3292481.
19. Araújo, de M.; Fangueiro, R.; Hong, H. Modelling and simulation of the mechanical behaviour of weft-knitted fabrics for technical applications: Part III: 2D hexagonal FEA model with non-linear truss elements. *Autex Res. J.* **2004**, *4*(1), 25-32. URL: https://www.researchgate.net/publication/288567971.
20. Cong, H.; Ge, M.; Jiang, G. Three-dimensional simulation of warp-knitted fabric. *Fibres Text. East. Eur.* **2009**, *3*(74): 66-69. URL: http://www.fibtex.lodz.pl/article19.html.